AD-A248 456

NTATION PAGE

Form Approved
OMB No. 0704-0188

1. AGENCY USE ONLY (Leave blank)	2. REPORT DATE	3. REPORT TYPE AND DATES COVERED
	18 Feb 92	Final 1 Jan 89 - 31 Dec 91

4. TITLE AND SUBTITLE
Millimeter-Wave Quasi-Optical Arrays

5. FUNDING NUMBERS
DAAL03-89-K-0041

6. AUTHOR(S)
Richard C. Compton

7. PERFORMING ORGANIZATION NAME(S) AND ADDRESS(ES)
Cornell University
School of Electrical Engineering
Phillips Hall
Ithaca, NY 14853-5401

8. PERFORMING ORGANIZATION REPORT NUMBER

9. SPONSORING/MONITORING AGENCY NAME(S) AND ADDRESS(ES)
U. S. Army Research Office
P. O. Box 12211
Research Triangle Park, NC 27709-2211

10. SPONSORING/MONITORING AGENCY REPORT NUMBER

11. SUPPLEMENTARY NOTES
The view, opinions and/or findings contained in this report are those of the author(s) and should not be construed as an official Department of the Army position, policy, or decision, unless so designated by other documentation.

12a. DISTRIBUTION/AVAILABILITY STATEMENT
Approved for public release; distribution unlimited.

12b. DISTRIBUTION CODE

13. ABSTRACT *(Maximum 200 words)*

Individual semiconductor devices can not output the power required for many future millimeter-wave systems. During this three year contract we have investigated an innovative way of coherently combining the outputs of a large number of semiconductor devices as a means of generating high power millimeter-wave signals. The combiner consists of a 2-D array of free running oscillators integrated into radiating antennas. Inter-element coupling in the array acts to lock all the elements together in-phase. Arrays of Gunn diodes and MESFETs have been built and will be described.

14. SUBJECT TERMS
Oscillator-Array, Spatial Power Combining

15. NUMBER OF PAGES
31

16. PRICE CODE

17. SECURITY CLASSIFICATION OF REPORT	18. SECURITY CLASSIFICATION OF THIS PAGE	19. SECURITY CLASSIFICATION OF ABSTRACT	20. LIMITATION OF ABSTRACT
UNCLASSIFIED	UNCLASSIFIED	UNCLASSIFIED	UL

Millimeter-Wave Quasi-Optical Arrays

Final Report

Richard C. Compton

February 18, 1992

U.S. ARMY RESEARCH OFFICE

CONTRACT NUMBER: DAAL03-89-K-0041

Cornell University

APPROVED FOR PUBLIC RELEASE;

DISTRIBUTION UNLIMITED.

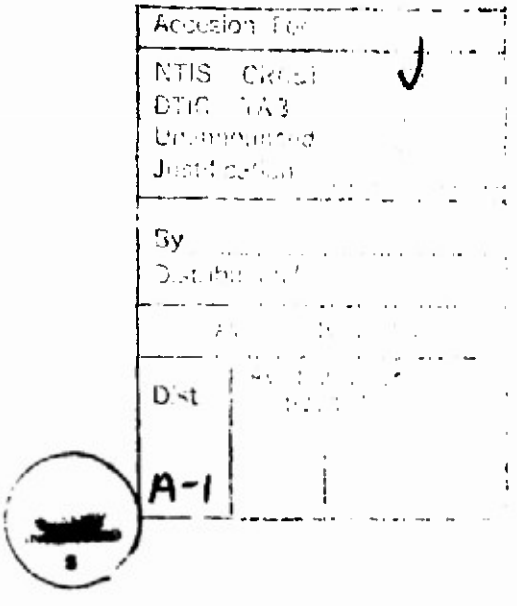

THE VIEWS, OPINIONS AND/OR FINDINGS CONTAINED IN THIS REPORT ARE THOSE OF THE AUTHOR AND SHOULD NOT BE CONSTRUED AS AN OFFICIAL DEPARTMENT OF THE ARMY POSITION, POLICY, OR DECISION, UNLESS SO DESIGNATED BY OTHER DOCUMENTATION.

TABLE OF CONTENTS

List of Illustrations

1. Introduction

The millimeter-wave spectrum holds promise for a wide range of existing and proposed military and civilian electronics systems. Satellite and terrestrial communications, remote sensing, and weather and air-traffic control radars all benefit from the small antennas, wide bandwidths, and high imaging resolution offered by millimeter-wave systems. Realization of the full potential of many such systems, however, awaits the development of practical and reliable high-power solid-state sources and amplifiers. At present, the generation and amplification of high-power millimeter-wave signals is dominated by vacuum-tube devices such as Gyrotrons and Travelling Wave Tubes (TWTs) [1]. This is undesirable in many applications due to the large size and weight of the systems, and the high-voltage power supplies required by the devices.

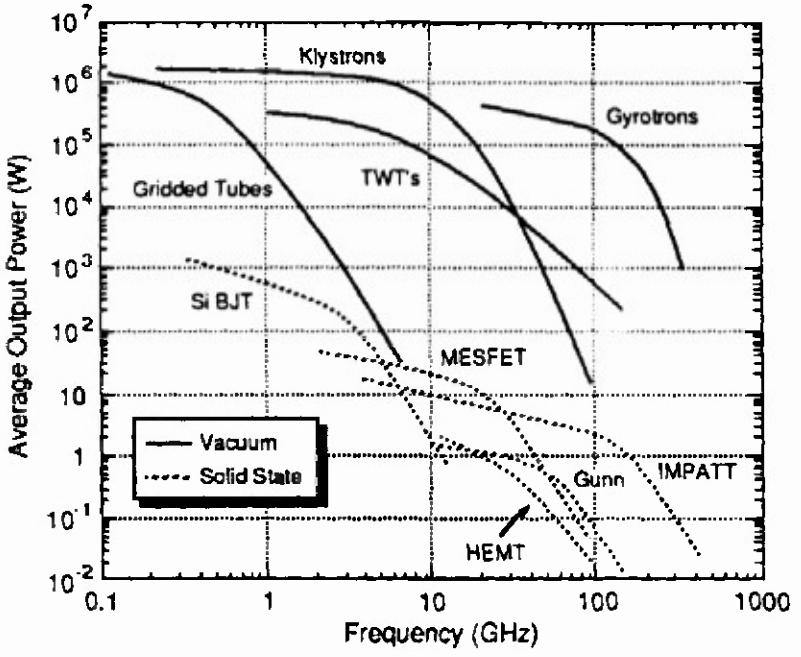

Figure 1 — Output power from a variety millimeter-wave sources. This figure shows clearly that large numbers of semiconductor devices are required to produce powers comparable with tubes.

In order to compete with millimeter-wave TWTs, solid-state transmitters must use large numbers of devices (figure 1). Several different approaches to the power-combining of multiple millimeter-wave devices have been reported [2]. Traditional combining techniques using hybrid 3 dB couplers, or large numbers of devices in a resonant cavity have fundamental limits regarding efficiency and the number of devices that can be combined. These limita-

tions arise from unavoidable circuit losses and/or the requirement of a small cavity in order to avoid multi-mode problems. Therefore these techniques are not suitable for combining large numbers of devices at millimeter-wave frequencies.

In recent years a planar quasi-optical approach has been suggested for combining the output powers of millimeter-wave sources [3]. In this approach a two-dimensional array of semiconductor devices is used, as in figure 2. Each device is integrated with a printed antenna, coupling it to the radiation field. In this way the power-combining takes place in free-space, and thus high combining efficiencies (close to 100%) are possible. The transverse dimension of quasi-optical systems can be quite large, which accommodates many devices. Devices need not be tightly packed together, so removal of waste heat is facilitated. Furthermore, where traditional combining techniques require many non-reciprocal elements to prevent device interaction, the quasi-optical arrays actually depend on the controlled interaction of the devices for proper operation. These arrays are expected to have application in a wide range of frequencies, up to the TeraHertz range using suitable devices [4].

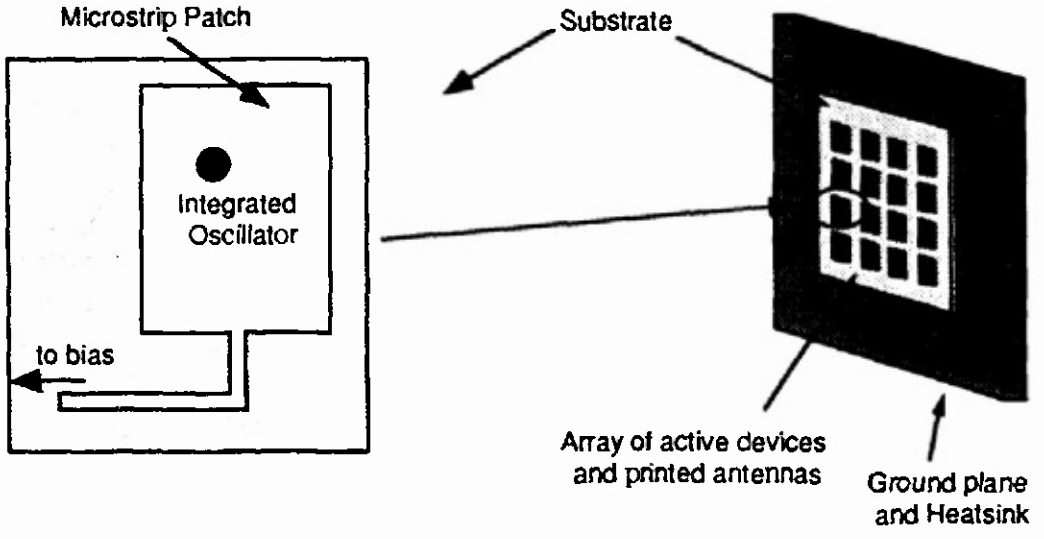

Figure 2 — Planar, solid-state millimeter-wave array. Large output powers may be obtained at millimeter-wave frequencies by quasi-optically combining the outputs of a large number of semiconductor devices.

Prior to the work performed in this grant there was one main quasi-optical array demonstration, originating with Rutledge at the California Institute of Technology, consisting of a distributed oscillator system in which devices are mounted in a periodic grid structure [5–8] and placed in an open quasi-optical cavity. It has been pointed out [9] that this approach

is analagous to a laser, in which the distributed oscillator system acts as the active gain medium, with the external reflectors providing the feedback. A 100-element MESFET array has been demonstrated successfully using this approach [10].

A second approach, originating from the work reported here, involves arrays of weakly-coupled individual oscillator elements [11]. This system forms a classical antenna array in which each radiating element is itself a free-running oscillator. The array elements are synchronized through weak mutual coupling mechanisms. The strength of the coupling between elements is limited to ensure that each element operates close to its free-running state, hence the operating frequency is solely determined by the design of the individual oscillator elements.

Coupled-oscillator arrays may have advantages over the distributed oscillator grids. For one, the array design is simplified by the use of weak coupling, since each element of the array is designed as a free-running oscillator and is only slightly perturbed from this state during operation. The technique is thus modular, as more elements can be added to increase the power without altering the operating frequency. It is also free of the multi-moding problem which plagues traditional combining techniques, because each element is designed to operate at only one frequency. Since the oscillators are electrically separated from their neighbors, they can be designed for maximum output power and efficiency. There is also more flexibility in the element spacing than with the grid approach, so that higher effective radiated powers per element are possible. Finally, the coupled oscillator architecture exhibits graceful degradation, meaning that if one oscillator fails the array will continue to operate normally, albeit with slightly deteriorated performance. This is in contrast to the oscillator grids, where failure of one device can lead to failure of an entire row or more.

2. Summary of the Most Important Results

2.1 Active Radiating Elements

The building blocks for the coupled oscillator arrays are the individual oscillator elements, consisting of an active device (Gunn, IMPATT, RTD, FET, etc.) integrated directly into a radiating element. Several novel architectures have appeared in the literature [12–16] which creatively incorporate an active device in a planar microstrip antenna. Important figures of merit are the output power, efficiency, and packing density. The experimental arrays described later were constructed using two different active microstrip patch antenna designs, one with a Gunn diode [12] and the other with a MESFET [16], as shown in figure 3. The patch antenna is a useful structure for this purpose, since the devices can be integrated vertically and heatsinking is facilitated by the ground plane.

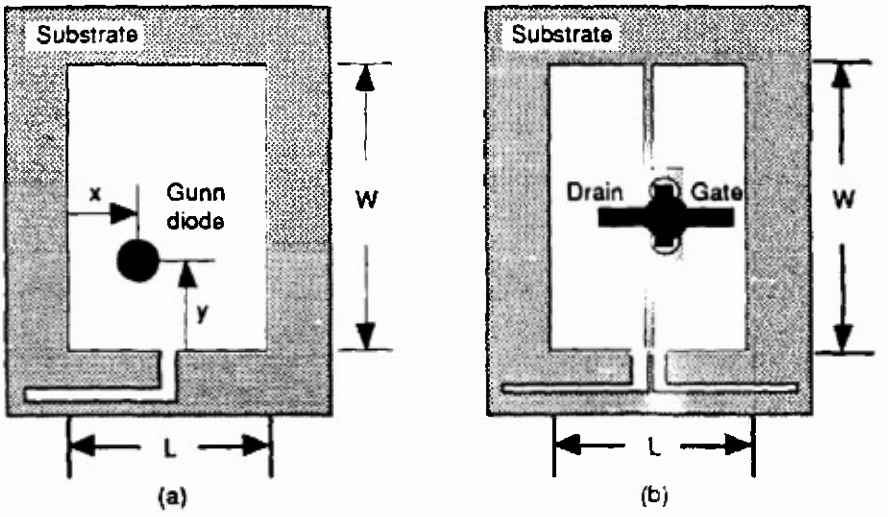

Figure 3 —Active patch antennas using two- and three-terminal devices. (a) A Gunn or Impatt diode is mounted between the ground plane and the patch. (b) An FET is mounted across the narrow gap, with source leads grounded through the substrate. Bias lines are also shown. These elements are simple to design and easy to fabricate, making them attractive for use in large arrays.

The Gunn/patch element was constructed using the topology of figure 3a. The device is located at the point where it's impedance is matched to that of the patch. This position can be found using a first-principles time-domain simulation of the device [17] and a suitable model for the patch input impedance (such as the cavity model). Alternatively a semi-

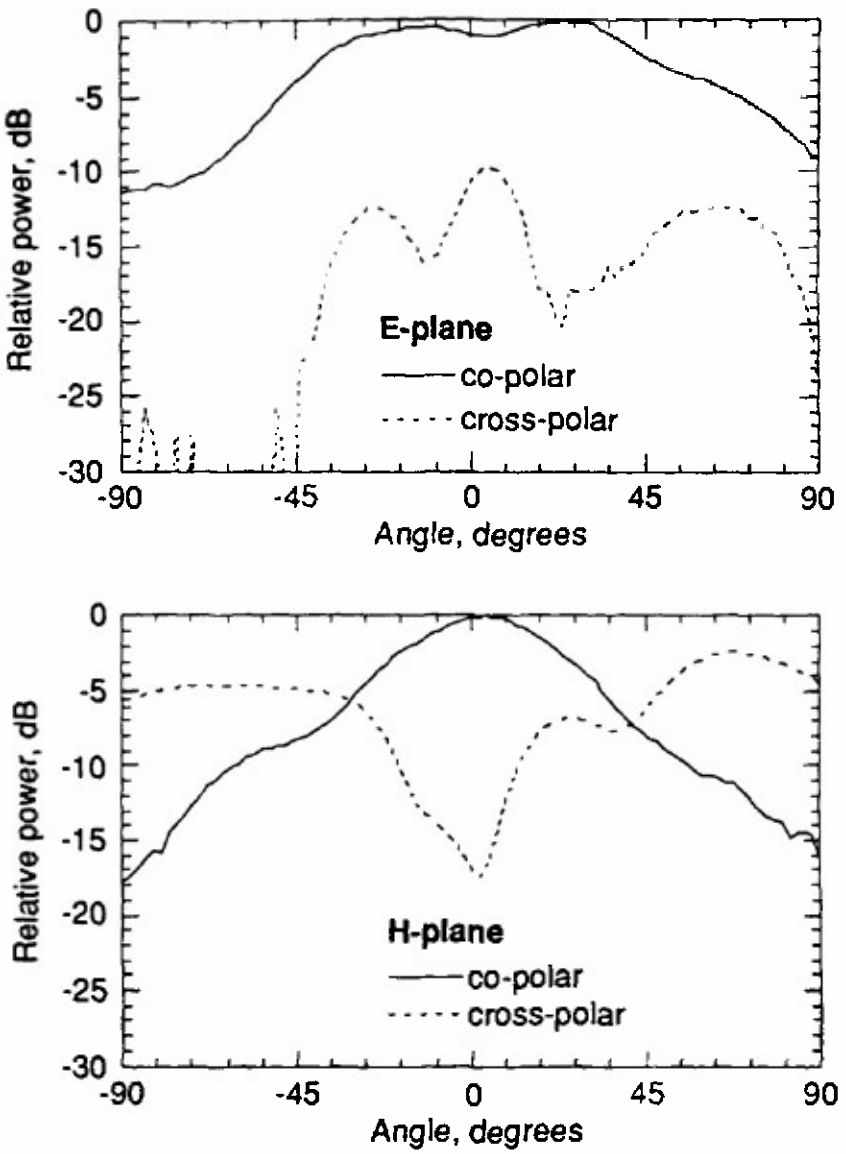

Figure 4 — E- and H-plane radiation patterns for a 7.6 GHz active patch using a Gunn diode. The patterns agree with expected patch behaviour, although the H-plane cross-polarization is abnormally large. This could be due to the large size of the packaged diode.

empirical approach can be used [18], where an approximate impedance is assumed for the device and the proper location is found using this impedance. The semi-empirical method is convenient for hybrid X-band circuits, but the more involved computer modeling is important for millimeter-devices which must integrated monolithically into the antenna and hence are more difficult and expensive to make. Bias is applied at a low impedance point on the patch.

A FET/patch element was also developed for power-combining arrays [16], and is shown in figure 3b. This structure is not a conventional patch antenna, since it uses two low-impedance microstrip lines coupled by a narrow gap. The device is mounted in a common-source configuration across this gap, with the source leads grounded through the substrate. The feedback capacitance from the gap is sufficient to make the device unstable (and hence useful as an oscillator), while the open circuited lines provide a good conjugate match to the load (radiation resistance). The FET/patch element has a demonstrated efficiency of 26%, but otherwise behaves similarly to the Gunn/patch element.

Typical radiation patterns for a Gunn/patch element are shown in figure 4. This element measured 0.45 by 0.65 inches, with the diode 0.15" from the edge, and was fabricated on 60 mil, $\epsilon_r = 4.1$ substrate. Commercially available low-power MA/COM packaged Gunn diodes (MA 49104) were used in this work. Typical bias was 12 volts @250 mA, with an overall DC-to-RF efficiency of 1%. Linear polarization and measured antenna patterns were consistent with expected patch behavior. The high cross-polarization in the H-plane measurement indicates excessive coupling to other patch modes, which is attributed to the large size of the diode package in relation to the antenna — this effect should be reduced in a monolithically fabricated array [12], since no bulky package would be used.

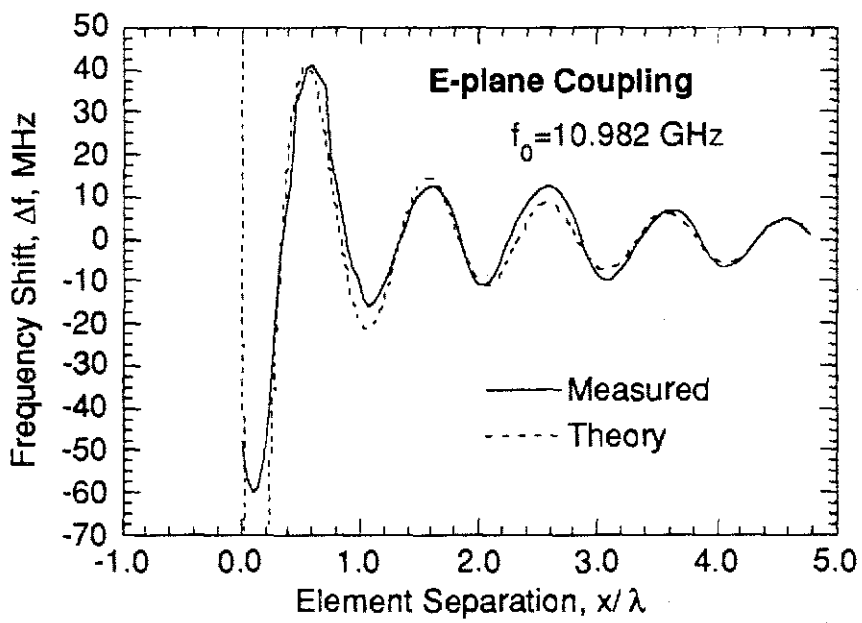

Figure 5 — Oscillator coupling measurement for a Gunn/patch in the E-plane. The theory curve is calculated as described in the text.

The tuning curves (frequency and output power versus bias voltage) for the circuit were very similar to other published measurements. Bias tuning can be used to compensate for small discrepancies between the elements, which is important because the proper operation of the array requires that the elements have nearly identical characteristics. For an array of elements, a partial reflector (such as a dielectric slab) positioned above the array facilitates the mutual injection-locking of the devices and helps establish the proper phase relationships between the elements. Figure 5 shows the measurements of a single Gunn/patch element when a dielectric slab is moved above the device.

2.2 Coupled Oscillator Theory

As part of the design of arrays an elegant treatment of oscillator coupling was developed based on Adler's equation for injection-locking [19]. An anlalysis of systems using using coupled or "inter-injection-locked" microwave oscillators has been previously published [19, 20]. These analyses are elegant but are impractical for power-combining arrays containing hundreds or thousands of elements. The theory gave us considerable physical insight into the design and operation of these arrays. This approach was motivated by recent work in low-frequency coupled oscillators [24,25]. In that work, an unusual mathematical model was postulated for the oscillator, which dissociates amplitude and phase dynamics. It was then argued that the steady-state behavior is a function of the phase dynamics alone, and after introducing a suitable coupling term, a compact analytical result for coupled oscillators was derived. However, the models were chosen without any correspondence to physical reality, and the coupling mechanism was assumed instantaneous, which is not a valid assumption at high frequencies. A summary of the theory is given in Appendix I.

The theory tell us that stable solutions require that the coupling signals between elements are sufficiently strong to lie in the locking range of the oscillators, and the coupling phase is a multiple of 2π. This theory has been confirmed by a series of array measurements.

2.3 Gunn Diode Arrays

The first experimental array of weakly coupled oscillators was a 16-element array using Gunn diodes, shown in figure 6 [10, 12]. The individual elements were designed semi-empirically, as described previously. This array design uses individual bias to each device, which was required due to device non-uniformities. Elements of the array are spaced a half free space

wavelength apart, a distance which was initially selected based on curves in [3]. The array was designed on a 60 mil substrate with $\epsilon_r = 4.1$.

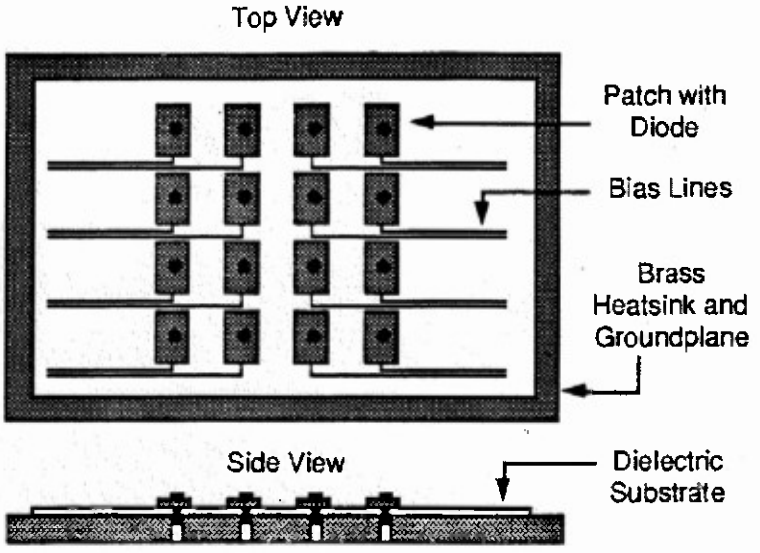

Figure 6 — Diagram of Gunn diodes mounted into a 4×4 array of microstrip patches. The brass block serves as a groundplane, heatsink, and DC bias return. Individual bias to each element is applied at an RF null.

Each diode was first biased, one at a time, to establish a common operating frequency. These individual biases were then applied simultaneously. Single frequency operation was verified with a spectrum analyzer, as shown in figure 7b. Spectra resembling figure 7a result when the elements are not all in synchronization (this effect has been fully explained using Adler's equation [22,23]). Slight differences in diode characteristics and diode placements made the simultaneous injection locking a delicate operation. As previously suggested, the addition of a 1 inch thick dielectric slab ($\epsilon_r = 4.0$) above the array facilitated the injection-locking.

The individual elements exhibited a frequency tuning from 9.5 to 10.0 GHz versus bias voltage. The best results for the array were obtained at a frequency of 9.6 GHz, which is within 4% of the design frequency. Sharp patterns in both the E- and H-plane corresponding to a directivity of 17 dB were measured at this frequency (figure 8), and indicate in-phase operation. Some frequency tuning was observed by adjusting the position of the dielectric slab, but this effect is limited to the maximum locking range of the array ($\approx$ 100 MHz) and also changes the radiation patterns substantially.

A maximum received power of 9.6 mW was obtained at a distance of 1.1 meters away from

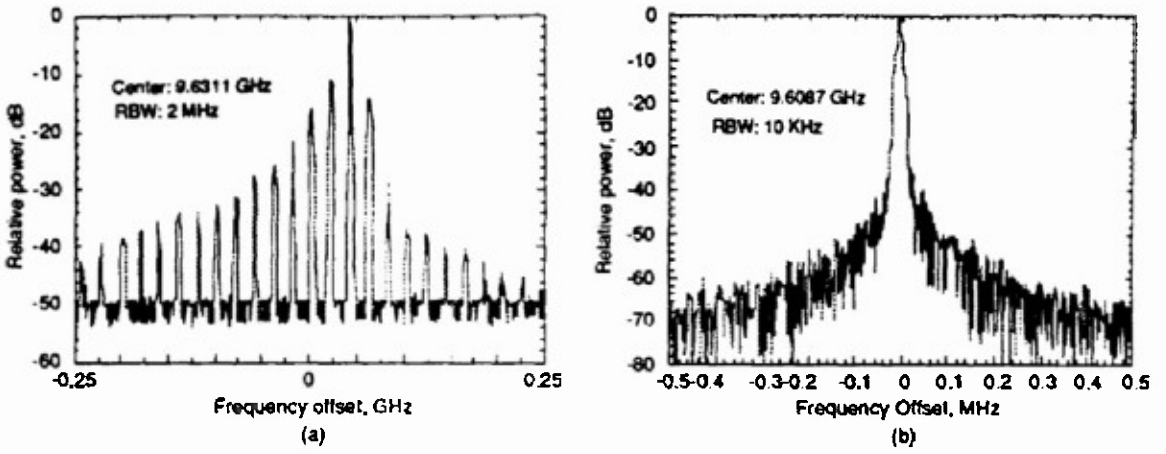

Figure 7 — (a) Spectrum of the Gunn array on the threshold of synchronization, and (b) at full synchronization. These measurements were made with the dielectric reflector in place.

the array, using a 19 dB pyramidal horn. The total radiated power, estimated from the measured E- and H-patterns, was 415 mW. The method of estimating total power from the principal radiation patterns is admittedly inaccurate, but based on comparisons with theoretical models we believe that the figure presented here may actually underestimate the total power by as much as 16%. This total power figure gives 26 mW per device, which is consistent with the 25 mW rating of the diodes — considerably more power could be obtained using higher-power devices. The above data corresponds to an EIRP of 22 Watts. The overall DC to RF conversion efficiency was low, typical of Gunn diodes, around 1%.

2.4 MESFET Arrays

While the Gunn diode array has demonstrated the concept of power-combining using the weakly-coupled oscillators, the low efficiency would be a major disadvantage in many applications. Much higher efficiency, larger tuning range, and better noise properties can be obtained using FET devices. Furthermore, the use of FETs also invites optical control control of the array [26].

The experimental MESFET array is depicted in figure 9. The individual element design was previously discussed, and each uses a general purpose Fujitsu device (FSX02). Half as many bias lines were used in this array design, with bias isolation between the elements provided using a 6-turn coil. The gate resistor was found neccessary to supress bias circuit oscillations. The array was fabricated on a 93 mil Duroid 5870 substrate ($\epsilon_r = 2.33$).

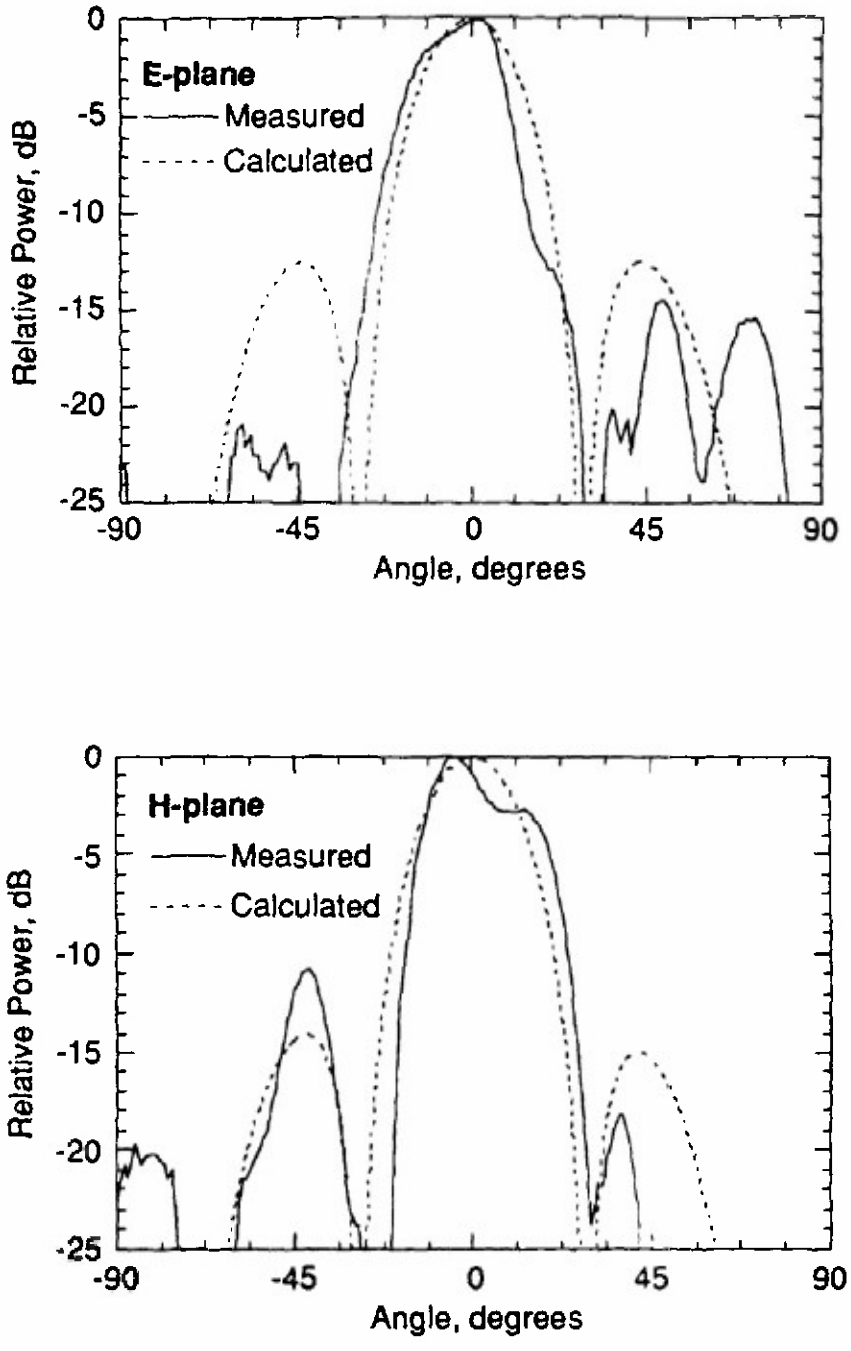

Figure 8 — Measured E- and H-plane patterns at 9.6 GHz for the active array of figure 6. The theoretical results are calculated by combining the pattern of a single patch with a 4×4 array factor. The dielectric slab above the array ($\epsilon_r = 4$) has a small effect on the patterns. Good qualitative agreement between the measured and calculated curves indicates that the elements are nearly in phase with similar amplitudes.

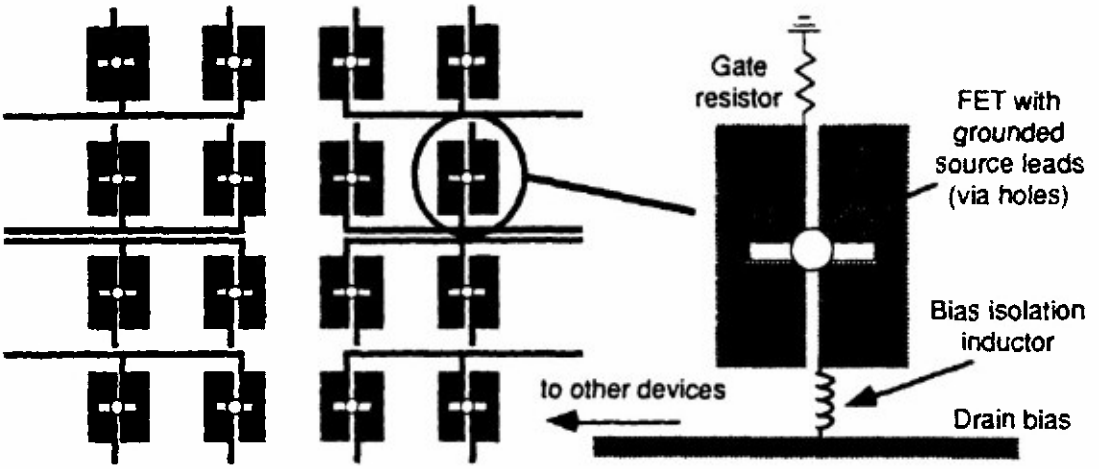

Figure 9 — Sketch of the array which uses Fujitsu fsx02 MESFETs, showing bias arrangement and individual element design. Elements measure 11 mm by 15 mm and the spacing of the elements is $0.67\,\lambda_0$ between centers. The bias inductor reduces element interactions along the bias line.

As with the Gunn array, the power-on sequence was to tune each group of elements individually to set a common operating frequency, and then apply DC power to all elements at once. Varying the reflector element spacing is then usually sufficient to enforce mutual synchronization. With single frequency operation verified at 8.27 GHz (within 3% of the 8 GHz design frequency) using a spectrum analyzer, the patterns were then measured. These patterns were found to be similar to the Gunn diode array and closely correspond to the expected pattern when the element are all in phase. Linear polarization measurements indicate low cross-polarization levels. A maximum received power of 1.4 mW at a distance of 2.23 m was measured using a 19 dB pyramidal horn, yielding an EIRP of 10 W. A total radiated power of 184 mW was estimated from the pattern measurements, giving 11.5 mW per device at 26% efficiency. The corresponding directivity is 17.2 dB. The results of the MESFET array are seen to be similar to that of the Gunn array, but with a much higher DC-to-RF efficiency, which makes it a more attractive design. Better efficiency and somewhat higher output power per device could be obtained by using gate bias to each element.

The MESFET array exhibited a broader tuning range than the Gunn array, approximately 400 MHz with varying reflector position. Much quieter operation was also observed, which is characteristic of FET's. The spectrum of the MESFET array is shown in figure 10, along with the spectrum when the array is externally-locked to an HP8350B sweeper (83592B

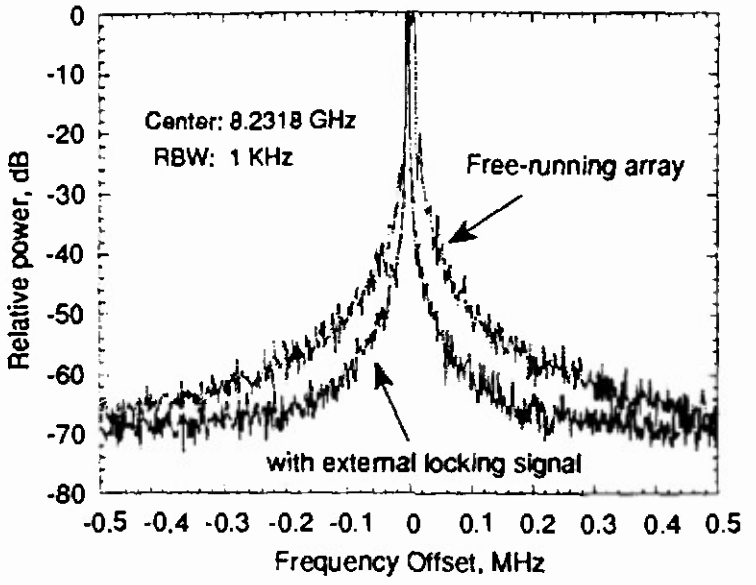

Figure 10 — Free-running and externally-locked spectra of the MESFET array. The locking signal was injected through a pyramidal horn, which illuminated the array from a distance of 1 meter.

plug-in). Phase noise of -78 dB /Hz at 100 kHz for the free-running case was measured using a spectrum analyzer.

2.5 Mode-locked Arrays

A mode-locked system is created when a number of different equally-spaced frequencies, or modes, are simultaneously produced and locked in phase with each other [27]. Duing the course of this contract, we discoverd that the weakly coupled arrays could be operated in an interesting mode-locked configuration. This mode-locking can be accomplished by arranging the frequencies of each oscillator in an array to produce a spectrum with equally spaced components, as shown in figure 11. The mutual coupling between the array elements then serves to lock the frequencies and phase-relationships together. This is a 'passive' mode-locking scheme, but 'active' mode-locking may be possible for increased stability and reliable operation.

Recent experimentation has revealed an additional feature of this system, namely that the pulse train is effectively scanned above the array as in a phased array source. Although previously unexpected, this phenomenon follows directly from the mode-locking theory and elementary array theory. The scan coverage is determined by the element spacing, while

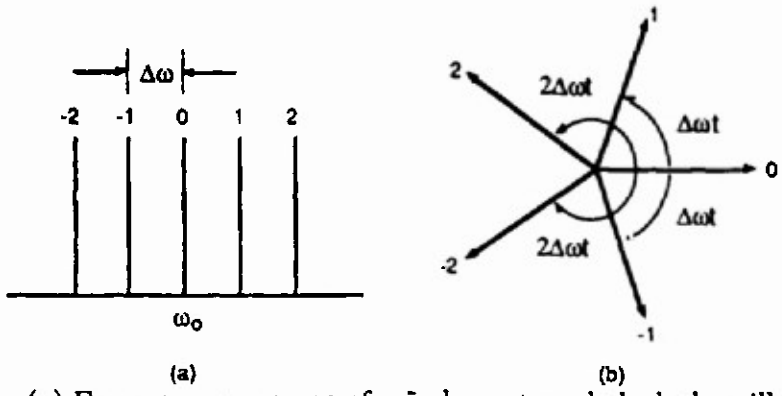

Figure 11 — (a) Frequency spectrum of a 5-element mode-locked oscillator array. (b) Phasor description in the complex plane at one instant of time.

the pulse repetition frequency is determined by the spacing of the spectral components. An oscillator array operated in this mode could potentially function as the transmitter in a phased-array radar application, *without the need for any phase shifters.* In addition, since the individual elements are operating in a CW mode, there are no thermal restrictions on the pulse repetition frequencies and no need for injection-priming of the array.

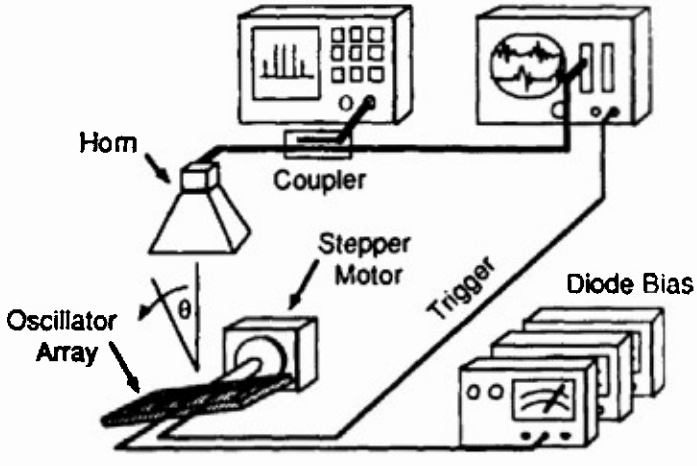

Figure 12 — Experimental setup for measuring the scanned pulse. A fixed receiving horn at the broadside position collects the output signal for observation on a spectrum analyzer and oscilloscope while the array is rotated.

The total electric field from an array of $M = 2m + 1$ oscillators spaced at frequencies $\omega = \omega_0 - i\Delta\omega$ with locked phases such that $\phi_i - \phi_{i-1} = \delta\phi$, $(i = -m, \ldots, m)$ can be written

as [27]

$$E(t) = E_0 \frac{\sin[M\Delta\omega t'/2]}{\sin[\Delta\omega t'/2]} \exp(j\omega_0 t) \tag{1}$$

where t' is the elapsed time from the point at which all the oscillators have the same phase, and E_0 is the amplitude, assumed identical, of each of the oscillators. Equation (1) represents a carrier at frequency ω_0 modulated by a train of pulses. The peak power of each pulse is $E_0^2 M^2$, so that an array of 10 elements would produce a peak power of 100 times that of a single element.

Preliminary measurements using a 5-element linear array at 10 GHz show promising results [28,29]. The experimental setup is illustrated in figure 12. A receiving horn is located at the broadside position, while a time-reference trigger signal at the pulse repetition frequency is derived by capacitively coupling to the bias lines on the array. The output signal from the horn is observed on a spectrum analyzer and a high-speed oscilloscope as the array is rotated in the scanning plane.

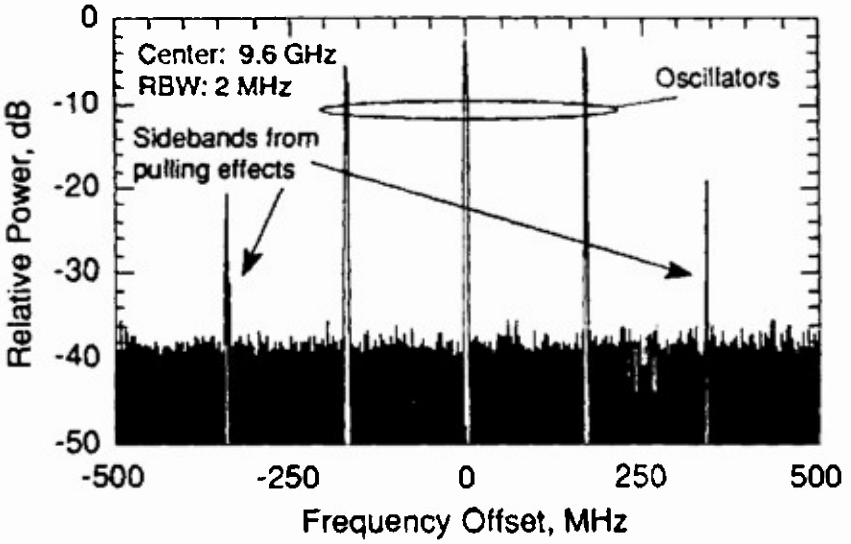

Figure 13 — Spectrum of three mode-locked microwave oscillators. Additional sidebands arise from frequency pulling effects [28].

An experimental observation of both the mode-locked pulse phenomena and the scanning was made by adjusting the oscillation frequencies of each element (using the bias supplies) to give equally spaced spectral components. This step was facilitated using the spectrum analyzer as shown in figure 13. Note from figure 13 that additional sidebands are produced

as a result of the mutual pulling effects. The pulse repetition rate is inversely proportional to the frequency difference, which was constrained by the locking range of the oscillators to 50 MHz or more.

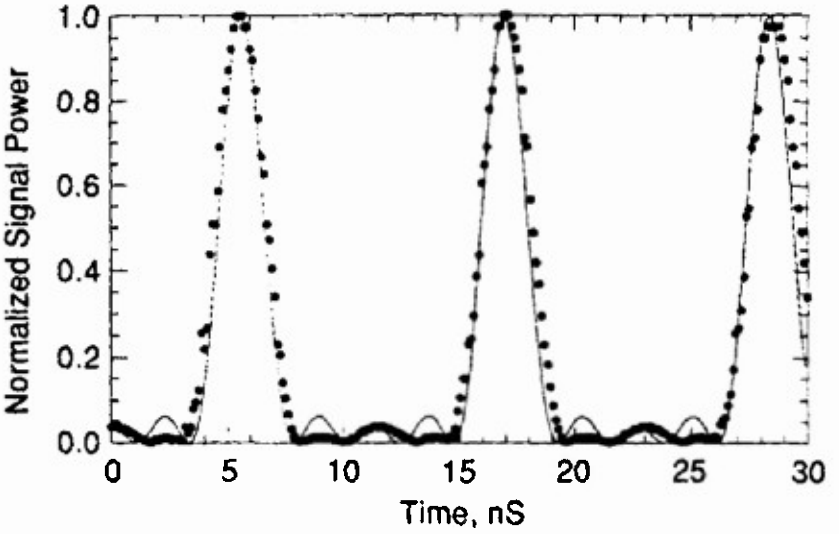

Figure 14 — Measured (•) and theoretical (solid line) time dependence of the output signal power envelope of five mode-locked oscillators.

Once the proper array spectrum was verified on the spectrum analyzer, a mode-locked pulse was clearly observed on the oscilloscope as shown in figure 14. In this figure, only the envelope of the output signal is shown for clarity. The theory curve presented in figure 14 is calculated from equation (1), and shows excellent agreement to the measurements.

When the array is rotated (as in figure 12) the pulse is observed to shift in time, corresponding to the pulse being scanned above the array. This is shown in figure 16 for three different scan angles. At large angles the pulse strength diminishes due to the radiation pattern of the individual patch antennas in the array.

3. List of Publications

Journal Publications

1. R. A. York, "Millimeter-wave power-combining with radiating oscillator arrays," PhD Thesis, Cornell University, August 1991.
2. A. Roberts and R. C. Compton, "A vector measurement scheme for testing millimeter-wave quasi-optical components," *International Journal of Infrared and Millimeter-Waves*, pp. 165-174, February 1990.

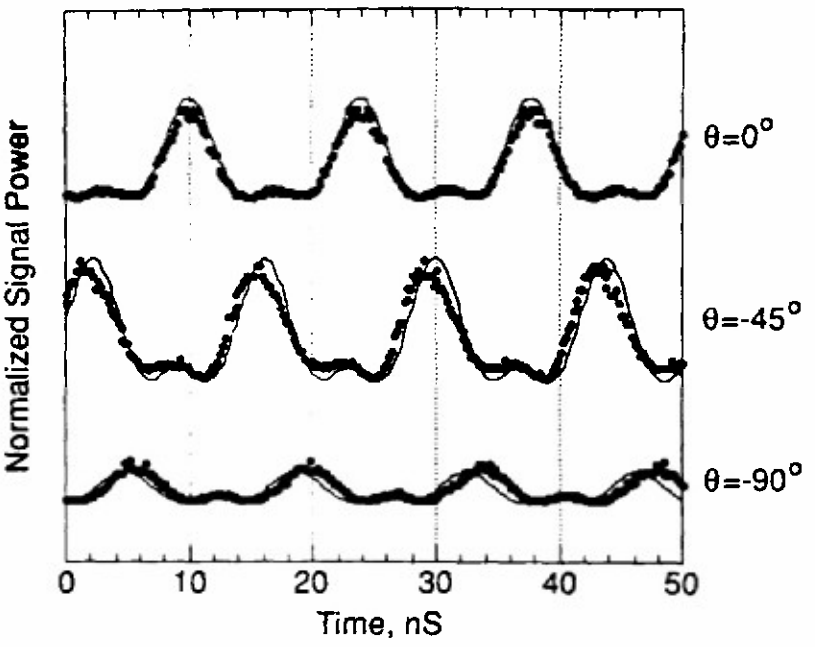

Figure 15 — Pulse waveforms for a three element active patch array at three scan angles, clearly demonstrating the automatic scanning of the output pulse.

3. R. A. York, R. D. Martinez, and R. C. Compton, "Active patch antenna element for array applications," *Electronics Letters* pp. 494–495, March 1990.
4. R. A. York, R. C. Compton, and B. J. Rubin "Experimental verification of the 2D rooftop modeling approach for modeling microstrip patch antennas," IEEE Transactions on Antennas and Propagation, pp. 690–693, May 1991.
5. R. A. York and R. C. Compton, "Quasi-optical power-combining using mutually synchronized oscillator arrays," IEEE Transactions on Microwave Theory and Techniques, pp. 1000–1009, June 1991.
6. R. A. York and R. C. Compton, " Mode-locked oscillator arrays," *The IEEE Microwave and Guided Wave Letters*, pp. 215–218, August 1991.
7. R. D. Martinez and R. C. Compton, "A general approach for the s-parameter design of oscillators with 1 and 2-port active devices," accepted for publication in the IEEE Transactions on Microwave Theory and Techniques, March 1992.
8. R. A. York and R. C. Compton, " Experimental observation and simulation of mode-locking phenomena in coupled-oscillator arrays," accepted for publication *Journal of Applied Physics*, March 1992.

Conference Publications

1. A. Roberts and R. C. Compton, "Bandpass filters for use in millimeter-wave quasi-optical systems," IEEE Antennas and Propagation International Symposium Digest, San Jose CA, pp. 1726–1729, June 1989.
2. A. Roberts, L. M. C. Sukamto, and R. C. Compton, "Millimeter-wave applications for planar arrays of ring resonators," Progress in Electromagnetics Research Symposium Proceedings, Cambridge MA, pp. 218-219, July 1989.
3. D. B. Rutledge, Z. B. Popovic, R. M. Weikle, M. Kim,K. A. Potter, R. A. York, and R. C. Compton, "Quasi-optical power-combining arrays," Invited Paper, MTT-S International Microwave Symposium, pp. 1201–1204, May 1990.
4. R. A. York and R. C. Compton, "A 4×4 array using Gunn diodes," IEEE Antennas and Propagation International Symposium, May 1990.
5. A. Roberts and R. C. Compton, "A vector measurement scheme for testing quasi-optical components," Fourth Symposium on Millimetre and Submillimetre Wave Research in Australia, February 1990.
6. B. J. Rubin, R. A. York, and R. C. Compton, "Accurate full-wave approach for modeling patch antennas," submitted to the 15TH International Conference on Infrared and Millimeter Waves.
7. C. Rehwinkle, M. M. Gitin, R. D. Martinez, R. A. York. K. R. Haselton, F. A. Wise, and R. C. Compton "Optical control of MESFET and HEMT millimeter/microwave circuits," presented at the 15TH International Conference on Infrared and Millimeter Waves, Orlando Dec 1990.
8. R. A. York and R. C. Compton, "TeraHertz power-combining with coupled oscillator arrays," Second International Symposium on space terahertz technology, February 1991.
9. R. C. Compton and R. A. York, "Integrated antenna/oscillator structures," Progress in Electromagnetics Research Symposium, Cambridge MA, July 1991.
10. R. A. York and R. C. Compton, "Design of weakly-coupled oscillator arrays," Progress in Electromagnetics Research Symposium, Cambridge MA, July 1991.
11. K. Y. Hur and R. C. Compton, "Millimeter-wave GaAs Schottky Barrier Photodiodes," presented at the 16TH International Conference on Infrared and Millimeter Waves, Switzerland August 1991.

4. Participating Personnel

Richard C. Compton	Assist Prof
Robert A. York	Ph.D. and Post Doc
(MS and PhD awarded during contract)	
Ann Roberts	Post Doc
Rene D. Martinez	Ph.D. Student
Mark M. Gitin	Ph.D. Student
Katerna Hur	Ph.D. Student

5. Report of Inventions

Pulsed Source Mode-Locked Oscillator Array

6. Bibliography

[1] J. W. Hansen, "U.S. TWT's from 1 to 100 GHz", *Microwave Journal, 1989 State-of-the-Art Reference*, pp. 179–193, Sept. 1989.

[2] K. Chang and C. Sun, "Millimeter-Wave Power-Combining Techniques," *IEEE Trans. on Microwave Theory Tech.*, vol. MTT-31, pp. 91–107, Feb. 1983.

[3] J. W. Mink, "Quasi-Optical Power-Combining of Solid-State Millimeter Wave Sources" *IEEE Trans. on Microwave Theory Tech.*, vol. MTT-34, pp. 273–279, Feb. 1986.

[4] M. J. Wengler, A. Pance, B. Liu, and R. E. Miller, "Quasioptical Josephson Oscillator", *IEEE Trans. on Magnetics* , vol. 27, no. 2, March 1991.

[5] Z. B. Popovic and D. B. Rutledge, "Diode-Grid Oscillators," *IEEE AP-S International Symposium, Proceedings*, pp. 442-445, May 1988.

[6] Z. B. Popovic, R. M. Weikle, M. Kim, K. A. Potter, and D. B. Rutledge, "Bar-Grid Oscillators", *IEEE Trans. Microwave Theory Tech.*, vol. MTT-38, pp. 225-230, March 1990.

[7] Z. B. Popovic, R. M. Weikle, M. Kim, and D. B. Rutledge, "A 100-MESFET Planar Grid Oscillator", *IEEE Trans. Microwave Theory Tech.*, vol. MTT-39, pp. 193-200, Feb 1991.

[8] Z. B. Popovic, M. Kim, and D. B. Rutledge, "Grid Oscillators", *Int. J. Infrared and Millimeter Waves*, vol. 9, pp. 647-654, July 1988.

[9] D. B. Rutledge, Z. B. Popovic, R. M. Weikle, M. Kim, K. A. Potter, R. A. York, and R. C. Compton, "Quasi-Optical Power Combining Arrays", *1990 IEEE MTT-S Int. Microwave Symp. Dig.* (Dallas), May 1990.

[10] R. A. York and R. C. Compton, "A 4×4 Array using Gunn Diodes", *IEEE Antennas and Propagation International Symposium* (Dallas), May 1990.

[11] R. A. York and R. C. Compton, "Quasi-Optical Power-Combining using Mutually Synchronized Oscillator Arrays", *IEEE Trans. Microwave Theory Tech.*, vol. MTT-39, pp. 1000-1009, June 1991.

[12] H. J. Thomas, D. L. Fudge, and G. Morris, "Gunn source integrated with microstrip patch", *Microwaves & RF*, pp. 87-89, Feb. 1985.

[13] T. O. Perkins, "Active Microstrip Circular Patch Antenna", *Microwave Journal*, pp. 110-117, 1987.

[14] K. Chang, K. A. Hummer, and G. K. Gopalakrishnan, "Active Radiating Element using FET Source Integrated with Microstrip Patch Antenna", *IEEE Trans. Microwave Theory Tech.*, vol. MTT-31, pp. 91-92, Sept. 1988.

[15] N. Camilleri and B. Bayraktaroglu, "Monolithic mm-wave IMPATT Oscillator and Active Antenna", *IEEE Trans. Microwave Theory Tech.*, vol. MTT-36, pp. 1670–1676, Dec. 1988.

[16] R. A. York, R. M. Martinez and R. C. Compton, "Hybrid Transistor and Patch Antenna Element for Array Applications", *Electron. Lett.*, vol. 26, pp. 494–495, March 1990.

[17] M. R. Lakshminarayana and L. D. Partain, "Numerical Simulation and Measurement of Gunn Device Dynamic Microwave Characteristics", *IEEE Trans. Electron Devices*,

vol. ED-27, no. 3, pp. 546–552, March 1980.

[18] K. Chang, K. A. Hummer, and J. L. Klein, "Experiments on Injection-Locking of Active Antenna Elements for Active Phased Arrays and Spatial Power Combiners," *IEEE Trans. on Microwave Theory Tech.*, vol. MTT-37, pp. 1078–1084, July 1989.

[19] K. D. Stephan, "Inter-Injection-Locked Oscillators for Power Combining and Phased Arrays", *IEEE Trans. Microwave Theory Tech.*, vol. MTT-34, no. 10, pp. 1017–1025, Oct. 1986.

[20] K. D. Stephan and W. A. Morgan, "Analysis of Interinjection-Locked Oscillators for Integrated Phased Arrays", *IEEE Trans. Antennas Propagat.*, vol. AP-35, no. 7, pp. 771–781, July 1987.

[21] R. Adler, "A Study of Locking Phenomena in Oscillators", *Proc. IRE*, vol. 34, pp. 351–357, June 1946; also reprinted in *Proc IEEE*, vol. 61, no. 10, pp. 1380–1385, Oct 1973.

[22] K. Kurokawa, "Injection-Locking of Solid-State Microwave Oscillators", *Proc. IEEE*, vol. 61, no. 10, pp. 1386–1409, Oct 1973.

[23] A. E. Siegman, *Lasers*, University Science Books, California, 1986. Chapter 19 offers an excellent discussion of injection locking, albeit in a different context than described here.

[24] B. Z. Kaplan and K. Radparvar, "Canonic coupling of sinusoidal oscillators: new results", *Int. J. Systems Sci.*, vol. 16, no. 10, pp. 1257–1263, 1985.

[25] B. Z. Kaplan and K. Radparvar, "Canonic Coupling of Oscillators in a Chain", *J. Franklin Inst.*, vol. 325, no. 1, pp. 49–60, 1988.

[26] C. Rehwinkle, M. M. Gitin, R. D. Martinez, R. A. York, K. R. Haselton, F. A. Wise, and R. C. Compton, "Optical Control of MESFET and HEMT Millimeter/Microwave Circuits", *15th International Conference on Infrared and Millimeter Waves*, (Orlando) Dec 1990.

[27] O. Svelto, *Principles of Lasers*, Plenum Press, New York, 1989.

[28] R. A. York and R. C. Compton, "Mode-Locked Oscillator Arrays", *IEEE Microwave and Guided Wave Letters.*, June 1991.

[29] R. A. York and R. C. Compton, "A Scanning Pulsed Source using Mode-Locked Oscillators", Submitted to the Journal of Applied Physics, June 1991.

Appendices

Appendix 1 Coupled Oscillator Theory

The assuption that individual oscillators in an array are only slightly perturbed from their free-running state by the presence of the other oscillators leads naturally to Adler's equation for injection locking [21–23],

$$\frac{d\phi_0}{dt} = -\frac{A_{inj}}{A_0}\frac{\omega_0}{2Q}\sin(\phi_0 - \psi_{inj}) + (\omega_0 - \omega_{inj}) \qquad (A.1)$$

where ϕ_0 = phase of oscillator, ψ_{inj} = phase of injected signal, ω_0 = free-running frequency of oscillator, ω_{inj} = frequency of injected signal from an external or neighboring oscillator, A_0 = free-running amplitude of oscillator (voltage), A_{inj} = amplitude of injected signal (voltage), and Q = the external Q of the oscillator circuit. The phase of the oscillator is defined relative to the injected signal frequency, so that the steady-state solution, $d\phi_0/dt = 0$, corresponds to the oscillator being frequency-locked to the injected signal. Adding the injected frequency to both sides of (A.1) and noting that $\omega = \omega_{inj} + d\phi_0/dt$ = the instantaneous frequency of the oscillator, yields

$$\omega = \omega_0\left[1 - \frac{A_{inj}}{A_0}\frac{1}{2Q}\sin(\phi_0 - \psi_{inj})\right] \qquad (A.2)$$

For mutually syncronized arrays, (A.2) must be modified to include the effects of coupling delay and several simultaneous injected signals. First, the coupling between individual oscillators can be expressed in terms of a complex coupling coefficient. This is just the scattering parameter s_{ij} of the circuit connecting the two oscillators i and j (reciprocity is assumed, $s_{ij} = s_{ji}$). The magnitude and phase of this coupling coefficient are written separately as $s_{ij} \equiv \lambda_{ij}\exp(j\Phi_{ij})$. Secondly, superposition is used to account for several simultaneously injected signals. Incorporating the above for a system of N oscillators gives a modified form of Adler's equation for the ith oscillator,

$$\omega = \omega_i\left[1 - \sum_{j\neq i}^{N}\frac{\lambda_{ij}}{2Q_i}\frac{A_j}{A_i}\sin(\phi_i - \phi_j + \Phi_{ij})\right] \qquad i = 1, 2, \ldots, N \qquad (A.3)$$

where the instantaneous frequency ω of oscillator i is the same for all oscillators in the system *at synchronization*. Equation (A.3) describes a set of equations which can be used to determine the steady-state of the system. If the free-running parameters are given, the unknowns are the phase differences and operating frequency of the array. Conversely one can solve for the frequencies and amplitudes which give a prescribed phase distribution.

Some simple analytical results can be derived from (A.3) by considering a linear chain of oscillators with only nearest neighbors interactions (the more general situation of a two-dimensional array is similar but notationally more complicated). Assuming that the coupling is the same between adjacent elements in the array, $\lambda_{ij} \equiv \lambda$ and $\Phi_{ij} \equiv \Phi$. Furthermore, let $Q \equiv Q_i$, $\lambda' \equiv \lambda/2Q$, $\rho_i \equiv A_{i-1}/A_i$, and $\Delta\phi_i \equiv \phi_i - \phi_{i-1}$. The set of governing equations becomes

$$\omega = \omega_i \left[1 - \lambda' \rho_i \sin(\Phi + \Delta\phi_i) - \lambda' \sin(\Phi - \Delta\phi_{i+1})/\rho_{i+1}\right] \qquad n = 1, 2, \ldots, N \qquad (A.4)$$

Note that $\rho_1 = 1/\rho_{N+1} = 0$. This is the same form obtained in [25], except for the presence of the coupling phase term. However this additional term renders the equations unsolvable by conventional linear techniques. To solve these equations, further assumptions must be made such as a small angle restriction where $\sin(\Delta\phi_i) \approx \Delta\phi_i$, or a nonlinear root-finding procedure could be used. For small numbers of elements, the equations can be solved analytically.

In general there are many possible phase distributions which satisfy this set of equations, but not all are stable solutions. Stability of these modes can be investigated using a perturbation analysis. Recalling that $\omega = \omega_{inj} + d\phi_i/dt$ a new differential equation is obtained,

$$\begin{aligned} \frac{d}{dt}\Delta\phi_i = {} & \omega_i \left[1 - \lambda' \rho_i \sin(\Phi + \Delta\phi_i) - \lambda' \sin(\Phi - \Delta\phi_{i+1})/\rho_{i+1}\right] \\ & - \omega_{i-1} \left[1 - \lambda' \rho_{i-1} \sin(\Phi + \Delta\phi_{i-1}) - \lambda' \sin(\Phi - \Delta\phi_i)/\rho_i\right] \end{aligned} \qquad (A.5)$$

The phase is then perturbed by a small amount by letting $\Delta\phi_i \rightarrow \Delta\phi_i + \delta_i$. After some algebra this leads to

$$\begin{aligned} & \frac{d}{dt}\delta_i = a_i\delta_{i-1} + b_i\delta_i + c_i\delta_{i+1} \qquad i = 2, 3, \ldots, N \\ \text{where} \quad & a_i = \lambda' \rho_{i-1} \omega_{i-1} \cos(\Phi + \Delta\phi_{i-1}) \\ & b_i = -\lambda' \omega_i \rho_i \cos(\Phi + \Delta\phi_i) - \lambda' \omega_{i-1} \cos(\Phi - \Delta\phi_i)/\rho_i \\ & c_i = \lambda' \omega_i \cos(\Phi - \Delta\phi_{i+1})/\rho_{i+1} \end{aligned} \qquad (A.6)$$

This is of the form of a matrix equation, $d\underline{\delta}/dt = \mathbf{A}\underline{\delta}$, where A is a tridiagonal matrix, and $\underline{\delta}$ is a column vector with elements δ_i. A stable solution for the phase distribution requires $\underline{\delta}$ to decay with time. This is satisfied when all the eigenvalues of **A** have negative real parts. In all of the numerical solutions of (A.4) and (A.6) which have been carried out so far, the stability criteria (A.6) has eliminated all but one or two of the possible modes given by (A.4). This observation has resisted an analytical justification so far. It has also been observed that for certain values of the coupling phase there are no stable modes of operation.

To illustrate the theory and derive some important qualitative results, consider a simple chain of four similar oscillators. From (A.4),

$$\begin{aligned}
\omega &= \omega_1 [1 - \lambda' \sin(\Phi - \Delta\phi_2)] \\
\omega &= \omega_2 [1 - \lambda' \sin(\Phi + \Delta\phi_2) - \lambda' \sin(\Phi - \Delta\phi_3)] \\
\omega &= \omega_3 [1 - \lambda' \sin(\Phi + \Delta\phi_3) - \lambda' \sin(\Phi - \Delta\phi_4)] \\
\omega &= \omega_3 [1 - \lambda' \sin(\Phi + \Delta\phi_4)]
\end{aligned} \tag{A.7}$$

assuming that the oscillator amplitudes are the approximately the same so that $\rho_i \approx 1$. This is usually a good approximation in practice. From (A.7), if the amplitudes are similar, then the final oscillation frequency of the array will lie within the locking range of each oscillator; that is, the locking ranges of every oscillator must overlap to some extent. Since these are weakly coupled oscillators, the locking bandwidth is small, hence the elements must be nearly identical to satisfy (A.7). It is important to note, from (A.2), that since the oscillator phase undergoes a 180° variation over the locking range, small differences in the free-running frequencies can have a large effect on the solution. Assuming perfectly identical oscillators ($\omega_1 = \omega_2 = \omega_3 = \omega_4$), gives

$$\begin{aligned}
\sin(\Phi - \Delta\phi_2) &= \sin(\Phi + \Delta\phi_2) + \sin(\Phi - \Delta\phi_3) \\
\sin(\Phi + \Delta\phi_2) + \sin(\Phi - \Delta\phi_3) &= \sin(\Phi + \Delta\phi_3) + \sin(\Phi - \Delta\phi_4) \\
\sin(\Phi + \Delta\phi_3) + \sin(\Phi - \Delta\phi_4) &= \sin(\Phi + \Delta\phi_4)
\end{aligned} \tag{A.8}$$

This shows that end effects will be important, at least for small arrays, since the elements on the periphery see quite different injection signals. There are many possible solutions to (A.8); for phase-coherent power-combining, of most interest is the solution for which $\Delta\phi_2 = \Delta\phi_3 = \Delta\phi_4 = 0$. For this solution, (8) is satisfied when $\Phi = n\pi$, where $n = 0, 1, 2 \ldots$. From the stability analysis, the following eigenvalue equation is obtained

$$\begin{vmatrix}
-2\cos\Phi - \epsilon & \cos\Phi & 0 \\
\cos\Phi & -2\cos\Phi - \epsilon & \cos\Phi \\
0 & \cos\Phi & -2\cos\Phi - \epsilon
\end{vmatrix} = 0 \tag{A.9}$$

The eigenvalues ϵ can have negative real parts only if $\cos\Phi > 0$, so a stable, in-phase mode is only possible if $\Phi = 0, 2\pi, \ldots$. If free-space coupling is predominant, this means that the elements must be spaced at mutiples of one wavelength. Such spacing is generally unacceptable because of grating lobes in the antenna patterns. Furthermore, it has been shown that close spacing is desirable for large arrays for efficient power combining [3].

Appendix 2. Mode-Locked Array Theory

For an array of resonant radiating structures, a very simple circuit model has been found to adequately predict experimentally observed effects. The model consists of an active device, such as a Gunn diode, embedded in a series resonant circuit. It is assumed that the active device can be modelled by an effective negative resistance, whose magnitude is amplitude-dependent but frequency-independent to first order. A schematic for this circuit is shown in figure 5, where an additional source is included for externally injected signals.

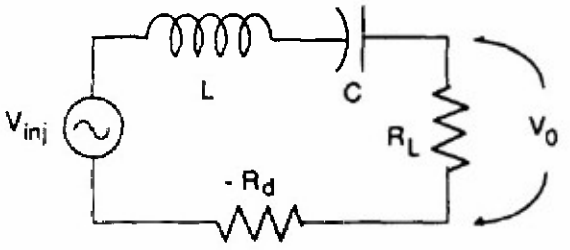

Figure 16 — Simple circuit model for a single oscillator. The device is represented by a lumped negative resistance. A single-tuned resonant circuit is assumed, so that harmonic effects will be minimal. The source V_{inj} accounts for interactions with neighboring oscillators.

The circuit equation corresponding to figure 16 is

$$V_{inj} = \frac{L}{R_L}\frac{dV_0}{dt} + \frac{1}{R_L C}\int V_0\,dt + V_0\left(1 - \frac{R_d}{R_L}\right) \qquad (A.10)$$

where V_0 is the output voltage amplitude and V_{inj} is the injected signal due to neighboring oscillators. For convenience, let $\delta(V_0) = 1 - R_d/R_L$, where the dependence of the negative resistance on amplitude has been explicitly written. If $V_{inj} = 0$, then the oscillation condition would require $\delta(V_0) = 0$, however when there is an injected signal present this parameter is non-zero to accommodate the additional energy being supplied to the circuit. For a series tuned circuit

$$\omega_0^2 = \frac{1}{LC} \qquad \frac{R_L}{L} = \frac{\omega_0}{Q} \qquad R_L C = \frac{1}{\omega_0 Q}$$

where Q is the quality factor of the passive resonating circuit. The Q-factor is assumed to be large enough ($Q > 10$) so that the output signal will be close to the natural resonant frequency of the circuit,

$$V_0 = A_0(t)\exp\{\jmath(\omega_0 t + \phi_0(t))\} = \tilde{A}_0 e^{\jmath\omega_0 t} \qquad (A.11)$$

Following van der Pol's approach (or the method of averages), the amplitude and phase variables are allowed to be slowly varying functions of time, leading to the set of equations

$$\frac{dA_0}{dt} = -\frac{\omega_0}{2Q}\delta(A_0)A_0 + \frac{\omega_0}{2Q}A_0 \,\mathrm{Re}\left\{\frac{V_{inj}}{V_0}\right\} \qquad (A.12a)$$

$$\frac{d\phi_0}{dt} = \frac{\omega_0}{2Q}\,\mathrm{Im}\left\{\frac{V_{inj}}{V_0}\right\} \qquad (A.12b)$$

Equation (A.12b) is recognized as Adler's equation for injection-locking.

The negative resistance appearing in (A.12), via the term $\delta(A_0)$, is a time-averaged value described by

$$R_d = \frac{1}{T}\int_0^T \frac{V_d(t)}{I_d(t)}\,dt$$

where V_d and I_d are the voltage and current at the terminals of the device. Consistent with the implicit assumptions of our circuit model, the simplest nonlinearity which yields a sinusoidal oscillation is a cubic relationship between the current and voltage, which gives an approximate expression for the amplitude dependence of negative resistance as $R_d(A) = a - bA^2$. The amplitude dependence of negative resistance is the mechanism responsible for the amplitude-limiting of any real oscillator. Normalizing this expression such that the free-running oscillations occur when $A_0 = 1$ gives

$$\delta(A_0) = -\mu(1 - {A_0}^2) \qquad (A.13)$$

where $\mu \equiv b/R_L$ is a parameter representing the oscillator. With this relation, (A.12) is seen to be closely related to the van der Pol equation. In the following discussions (A.13) will be used to represent the amplitude dependance, and μ is taken as an empirically determined quantity.

For a coupled system of such oscillators, the coupling between elements can be described by a complex coupling coefficient, κ, where

$$\kappa_{ij} \equiv \lambda_{ij}\exp(-j\Phi_{ij})$$

for the coupling between oscillators i and j in the system. Reciprocity is assumed in the following discussion ($\kappa_{ij} = \kappa_{ji}$). The injected signal seen by the ith oscillator is then

$$V_{inj} = \sum_{\substack{j=1 \\ j\neq i}}^{N} \kappa_{ij}V_j$$

where N is the number of oscillators in the system and V_j is the output signal of the jth oscillator. With A_i and ω_i denoting the amplitude and free-running frequency of the ith oscillator, and using the instantaneous phase $\theta_i \equiv \omega_i t + \phi_i$, a system of equations describing the coupled oscillator dynamics can be derived, giving

$$\dot{A}_i = -\frac{\omega_i}{2Q}\delta(A_i)A_i + \frac{\omega_i}{2Q}\sum_{\substack{j=1 \\ j\neq i}}^{N} \lambda_{ij} A_j \cos(\Phi_{ij} + \theta_i - \theta_j)$$

$$\dot{\theta}_i = \omega_i - \frac{\omega_i}{2Q}\sum_{\substack{j=1 \\ j\neq i}}^{N} \lambda_{ij}\frac{A_j}{A_i}\sin(\Phi_{ij} + \theta_i - \theta_j) \qquad i = 1, 2, \ldots, N \qquad (A.14)$$

Experiments have indicated that nearest-neighbor interactions among oscillators in a radiatively coupled system are the most important, as depicted in figure 17. Assuming the coupling to be the same between adjacent oscillators in the system yields $\lambda_{ij} \equiv \lambda$ and $\Phi_{ij} \equiv \Phi$. Using this simplification, and writing out $\delta(A_i)$ explicitly, simplifies (A.14) to

$$\dot{A}_i = \frac{\omega_i}{2Q}\mu(1 - A_i{}^2)A_i + \lambda\frac{\omega_i}{2Q}\sum_{\substack{j=i-1 \\ j\neq i}}^{i+1} A_j \cos(\Phi + \theta_i - \theta_j)$$

$$\dot{\theta}_i = \omega_i - \lambda\frac{\omega_i}{2Q}\sum_{\substack{j=i-1 \\ j\neq i}}^{i+1} \frac{A_j}{A_i}\sin(\Phi + \theta_i - \theta_j) \qquad i = 1, 2, \ldots, N \qquad (A.15)$$

The relative phase differences between the oscillators is of most interest, so let $\Delta\theta_i \equiv \theta_i - \theta_{i-1}$ and $\Delta\omega_i \equiv \omega_i - \omega_{i-1}$. Furthermore, note that the equations (A.14) are only valid to first order in $1/Q$, and for $\Delta\omega_i \ll \omega_i$. Under these assumptions the quantity $\omega_i/2Q$ is approximately the same for every oscillator. Defining $\mu' \equiv \omega_0/2Q$ and $\lambda' \equiv \omega_0/2Q$, where ω_0 is an average frequency for the oscillator ensemble, yields

$$\dot{A}_i = \mu'(1 - A_i{}^2)A_i + \lambda' f_i(\mathbf{A}, \Delta\theta) \qquad i = 1, 2, \ldots, N \qquad (A.15a)$$

$$\Delta\dot{\theta}_i = \Delta\omega_i + \lambda' g_i(\mathbf{A}, \Delta\theta) \qquad i = 2, 3, \ldots, N \qquad (A.15b)$$

where $f_i(\mathbf{A}, \Delta\theta) = A_{i-1}\cos(\Phi + \Delta\theta_i) + A_{i+1}\cos(\Phi - \Delta\theta_{i+1})$

$$g_i(\mathbf{A}, \Delta\theta) = \frac{A_{i-2}}{A_{i-1}}\sin(\Phi + \Delta\theta_{i-1}) + \frac{A_i}{A_{i-1}}\sin(\Phi - \Delta\theta_i) - \frac{A_{i-1}}{A_i}\sin(\Phi + \Delta\theta_i) - \frac{A_{i+1}}{A_i}\sin(\Phi - \Delta\theta_{i+1})$$

and where $A_0 = A_{N+1} = 0$ is assumed. For $\lambda = 0$ the oscillators are uncoupled, and (A.15) reduces to a set of isolated limit cycle oscillators with amplitudes $A_i = 1$ and frequencies ω_i.

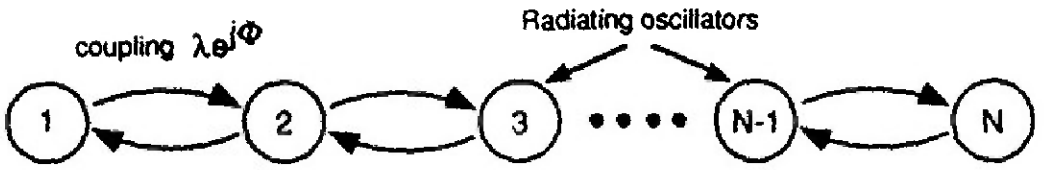

Figure 17 — A chain of radiatively-coupled oscillators, with bilateral coupling between nearest neighbors.

Equation (A.15b) can be considered a modified version of Adler's equation. For loose coupling and a narrow distribution of oscillator frequencies, the amplitudes will remain close to the free-running values, and the oscillator dynamics will be essentially governed by (A.15b). In this case all of the oscillators in the system may lock to a single frequency, associated with stable, fixed points of (A.15b). The parameter λ' in (A.15) is closely related to the locking bandwidth of the oscillators. Thus for widely varying oscillator frequencies such that $\Delta\omega_i > \lambda'$, the oscillators may not lock to a single frequency. In this case the amplitude dynamics described by (A.15a) can not be ignored, and both A_i and $\Delta\theta_i$ will be functions of time in the steady-state. This is the regime in which mode-locking can occur.